2011 American Control Conference
on O'Farrell Street, San Francisco, CA, USA
June 29 - July 01, 2011

Parameter Varying Control of an MR Damper for Smart Base Isolation

Farzad A. Shirazi, Karolos M. Grigoriadis and Gangbing Song

Abstract— **This paper presents a parameter varying control of a magnetorheological (MR) damper with stiction effect and its application to seismic protection of a model two-story structure. This semi-active device is utilized to reduce the vibrations of the model structure due to earthquake excitations. A modified Bingham model is used to capture the nonlinear hysteretic dynamics of the MR damper including the stiction effect. The parameters of the model are identified by solving a nonlinear optimization problem. The Bingham model is considered because of its simple structure to be used in linear parameter varying (LPV) controller design. The model is verified experimentally showing an acceptable level of accuracy. The second part of the paper addresses the LPV controller design to command the MR damper to suppress the structural vibrations. The LPV controller is designed for the combined structure and MR damper based on the Bingham model. The scheduling parameter is chosen to be damper velocity which is obtained by measurement. An optimal passive damping design is also obtained for comparison purposes. The performance of the controller is compared with the optimal passive damping case for El Centro and Northridge earthquakes with different intensities. The experimental results show the improved performance of the LPV controller design approach in terms of the maximum acceleration and the RMS values of the structure response.**

I. Introduction

The semi-active vibration control employing magnetorheological (MR) dampers has been the topic of research in a wide range of applications from smart base isolation and damping to car suspension systems and medical prosthetic joints [2], [16], [18]. MR dampers exhibit a highly nonlinear hysteretic dynamics, which makes them difficult to be accurately modeled and effectively controlled. Different static and dynamic models have been presented and reviewed in the literature such as Bingham model, LuGre friction model, Bouc-Wen model and polynomial models [3], [6], [15]. As the aforementioned models are mathematical models, parameter identification is required to determine the corresponding values of the parameters for a given MR damper. A recursive least square (RLS) method has been used as a common tool to determine the parameters of the models whose dynamics are linear in the parameters [7]. Other approaches consist of formulating a nonlinear optimization problem and then solving the problem to find the best match between data and the model output. An adaptive identification algorithm has been proposed by Terasawa *et al.* applied to LuGre and Bouc-Wen models, which copes with uncertainties in the MR damper model parameters and shows an acceptable level of accuracy in online identification [12], [13].

The authors are with Mechanical Engineering Department, University of Houston, Houston, TX 77204. Email: fashiraz@mail.uh.edu

Different strategies have been investigated to control the nonlinear hysteretic behavior of MR dampers. H_2/LQG control designs are well-known in the literature integrated with a clipped-optimal algorithm or an inverse model of the MR damper [12], [16], [18]. The clipped-optimal controller employs a desired optimal control force that is determined using linear optimal controllers and then switches accordingly between zero and maximum control effort to accommodate the required damping force [3], [17]. Semi-active control based on state-feedback H_∞ controller and bilinear H_∞ design have also been studied to suppress the structural vibration due to external disturbances [6], [12]. Since force cannot be directly commanded to the damper, an inverse model of the MR damper is used to convert the control force to the corresponding voltage. This voltage is the input to the MR damper which produces the required damping force to attenuate the vibrations of the structure. In a series of recent work, semi-active suspension control based on linear parameter varying (LPV) design was studied considering the combined MR damper and suspension system [2], [10]. The latter work considers a static model for damper and an LPV design with two scheduling parameters.

In this work, we propose a modified Bingham model to capture the dynamic behavior of an MR damper with stiction effect. The parameters of the Bingham model are identified by solving a nonlinear optimization problem. The obtained model is verified experimentally for different operating conditions. The identified MR damper is used to attenuate the vibration of a two-story model structure. An LPV controller is designed to control the combined structure and MR damper. The Bingham model, that has a simpler structure than other existing models, is used to capture the nonlinear dynamics of the damper. A classical anti-windup scheme is also considered to resolve the saturation issue due to actuation constraints. For comparison purposes, an optimal passive damping design is also obtained for a constant voltage of the MR damper in response to different intensties of El Centro earthquake. The maximum and root mean square (RMS) structural responses due to El Centro and Northridge earthquakes are compared for the LPV controller and the optimal passive damping design.

II. Experimental Setup

In this section, the experimental setup for the MR damper parameter identification and smart base isolation is briefly presented. The experimental setup consists of the following major parts: the shaking table and its driving components, a two-story model building, the MR damper, and sensors for displacement and acceleration measurements. The shaking

978-1-4577-0079-8/11/$26.00 ©2011 AACC

table used in this study is the Shaker II by Quanser company. The capabilities of the table are $\pm$7.5 cm maximum displacement, $\pm$83.8 cm/s peak velocity, and $\pm$24.5 m/s^2 peak acceleration with a 930 kg bearing load carrying. The operational bandwidth of the table is 0-20 Hz.

The displacement of the base and first floors are measured by two LB-70 series laser displacement sensors by KEYENCE company. The measurement range is 100 mm $\pm$40 mm with fastest response time of 0.7 ms. Accelerations of the second and the base floors are captured by MEMS accelerometers attached to each floor by wax. The type of accelerometer used is ADXL203EB Rev.0 by Analog Device company. The measurement range is $\pm$1.7 g, and the sensitivity is 1 mg in 60 Hz satisfying the requirements of the experiment, where $g = 9.81$ m/s^2 is the standard gravity. The dSPACE board DS1104 RD, with controller and communication board CLP 1104, is used as the data acquisition system. This board is linked with Matlab/Simulink via AD and DA converters and controls input and output signals in real-time. Furthermore, an Agilent 6542A programmable power supply is connected to the dSPACE board output to amplify the voltage for the MR damper. The sampling rate is set to be 500 Hz.

The MR damper under study is a custom-made device in the Smart Material and Structure Laboratory (SMSL) at the University of Houston. This device is a sponge-type damper which provides a stiction effect which should be taken into account in parameter identification and controller design. The damper consists of a magnetic coil, MR fluid and a sliding bar. The coil is excited by the voltage applied to the MR damper which increases the viscosity of MR fluid and consequently the force exerted on the sliding bar. The amount of force produced is proportional to the area of active MR sponge that is exposed to the magnetic field. The MR damper is excited by voltages up to 8V (0.55 A). The MR damper is attached between the base and a fixed point on the table to reduce the vibration of the structure. The damper stroke is $\pm$2 cm and it can approximately produce a maximum force of 10N in a voltage of 8V. Fig. 1 illustrates the experimental setup in the lab. The structure under study is a base-isolated

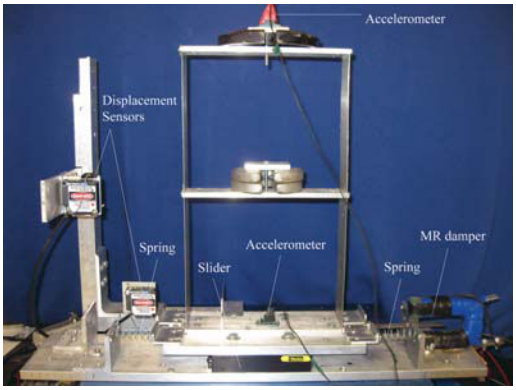

Fig. 1. MR damper experimental test bed

two-story model building. The structure is supported by a slider with low friction providing the base isolation. The base mass consists of the slider mass and a $205.7\times50.69\times6.51$ mm^3 aluminum plate. The mass of the first and second floors consist of the same aluminum plate and additional weights. The side plates are aluminum beams with dimensions of $17.60\times50.69\times0.75$ mm^3. Two springs with total stiffness of 1057 N/m are symmetrically attached to the base mass to restrict the base drift. The modal parameters of the structure are experimentally obtained by subspace-based identification method in a previous study at SMSL. The identified mass, stiffness and damping matrices of the structure are as follows

$$\mathscr{M} = \begin{bmatrix} 1.958 & 0 & 0 \\ 0 & 1.258 & 0 \\ 0 & 0 & 1.212 \end{bmatrix} [\mathtt{kg}],$$

$$\mathscr{C} = \begin{bmatrix} 1.281 & -0.487 & 0 \\ -0.487 & 1.325 & -0.599 \\ 0 & -0.599 & 0.829 \end{bmatrix} [\mathtt{N.s/m}],$$

$$\mathscr{K} = \begin{bmatrix} 2275.6 & -1218.6 & 0 \\ -1218.6 & 2716.3 & -1497.7 \\ 0 & -1497.7 & 1497.7 \end{bmatrix} [\mathtt{N/m}]$$

where the natural frequencies of the system are 2.1 Hz, 5.48 Hz and 9 Hz. The stiffness and damping coefficients corresponding to the base floor include the stiffness of the springs attached to the base and damping effect of the slider, respectively. A damping ratio of 1% has been assumed for all the structural modes. The proportional damping matrix has been obtained from $\mathscr{C} = a_0\mathscr{M} + a_1\mathscr{K}$, where a_0=0.1893 and a_1=0.0004.

III. Parameter Identification of the MR Damper

MR dampers are highly nonlinear devices and possess hysteretic characteristics. The MR damper under study is a custom-made damper showing some level of stiction effect. The friction phenomenon can have a major impact on the performance of a semi-active device. It is desirable to have an accurate model of the MR damper dynamics including stiction to improve the closed-loop system performance of the system in a model-based controller design. There are different models in the literature describing the hysteretic dynamics of the MR dampers ranging from simple Bingham model to the more complicated modified Bouc-Wen model. The accuracy of these models have been compared in [15]. As a rule of thumb, the more complicated models provide more accuracy. In this section, we develop a modified Bingham model to predict the frictional hysteretic behavior of the damper. The proposed model provides an acceptable level of accuracy with low complexity compared to other existing models.

A. Modified Bingham Model for MR Damper

The following Bingham-based model is proposed which considers the damping force decrease with increasing velocity.

$$F_{mr} = (f_a + f_b v)\,\mathtt{sign}(\dot{x}) + (c_0\dot{x} + c_{0v}\dot{x}v)e^{-(\frac{\dot{x}}{v_0})^2} \quad (1)$$

where the variables and parameters are defined as:
F_{mr}: Damper force when in motion (N)
v: Input voltage (V)
f_a: Coulomb frictional force (N)
f_b: Coulomb frictional force influenced by voltage v (N/V)
c_0: Viscous damping coefficient (N.s/m)
c_{0v}: Viscous damping coefficient influenced by voltage v (N.s/(m.V))
v_0: Normalizing velocity (m/s)

In this model the viscous damping coefficient is assumed to be linearly dependent on the input voltage v and all the parameters are positive. This model is valid for non-zero velocities. Here, we are only concerned with the static force at which the sliding bar of the damper starts moving. This force is dependent on the voltage and has been considered in the model (the term before the sign function). It is also noted that when the velocity is approximately zero, the control effort is set to zero.

The exponential term provides us with two effects: (i) the flattening effect expected at high velocities, and (ii) stiction effect in low forces. The first effect is physically motivated by the change of the damping characteristics as the velocity increases due to more lubricant being forced into the interface [9]. The second effect is more significant in low forces in which bumpy responses are observed in velocities close to zero. Different dependencies of the model terms on the exponential function were investigated which finally led to the proposed model.

It is common in practice to identify the damper dynamics in a separate setup and then attach it to the structure for vibration mitigation. In our case, we perform both identification and control experiments on the same setup which helps reduce the experimental effort. The parameter identification is performed by exciting the structure with a chirp signal from 1 to 10Hz with varying amplitude for 70 seconds. Indeed, the velocity input of the damper is the response of the structure to the chirp signal at the base floor which is rich enough to identify the damper dynamics. Specifically, the excitation signal should contain the frequencies close to natural frequencies of the structure under study, since the MR damper is expected to operate in these frequencies. The excitation voltage is considered to be a 2Hz sinusoidal signal with a peak-to-peak amplitude of 5V. The length of the data for identification should be long enough to let the structure respond to the exciting frequencies in an appropriate amount of time.

The MR damper force is not measured directly, but it is calculated from the base and first floor displacement and base acceleration readings with appropriate filtering. All the signals are low pass filtered within 18Hz which is twice the third natural frequency of the structure. The parameters of the model are determined by solving a nonlinear optimization problem which minimizes a quadratic error cost function between the measured and estimated output force. The solution of this optimization problem is dependent on the initial values of the parameters. Here, the solution with the minimum possible error is sought using varying initial conditions which results in the following values of the parameters:
$f_a = 0.35$ N, $f_b = 0.05$ N/V, $c_0 = 26.7$ N.s/m, $c_{0v} = 3.1$ N.s/m.V and $v_0 = 0.50$ m/s.

The identification results for the chirp velocity input and 2 Hz sinusoidal voltage is shown around the second mode of the system in Fig. 2 for the modified and standard Bingham models. The identification results are considered to be accurate enough to be used for control design. The

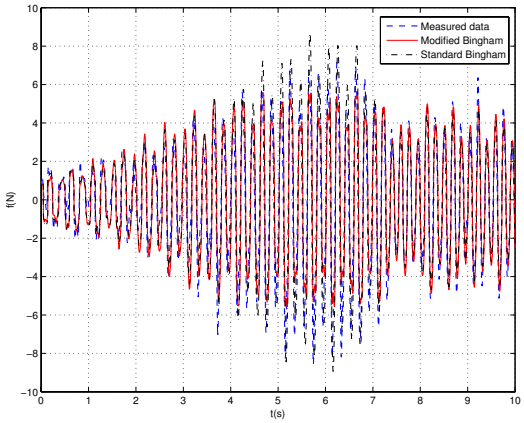

Fig. 2. Identification results using chirp velocity excitation for modified and standard Bingham models

parameters of the standard Bingham model are obtained by least square (LS) method. We observe that the RMS error of the modified model is about to 5% smaller than the standard model which demonstrates the benefit of the proposed modification.

IV. Controller Design for MR Damper Actuation

In this section, the dynamic equations of the structure including the MR damper are firstly presented and an optimal passive damping is obtained for different intensities of the El Centro earthquake. Subsequently, an LPV controller based on the modified Bingham model is introduced and designed for the combined structure and MR damper.

A. Dynamic Equations of the Structure with MR Damper

The dynamic equations of motion for the structure including the MR damper is expressed as follows:

$$\mathscr{M}\ddot{q} + \mathscr{C}\dot{q} + \mathscr{K}q = \Gamma F_{mr} - \mathscr{M}\Lambda\ddot{x}_g \tag{2}$$

where $q = [x_b \;\; x_1 \;\; x_2]^T$, $\Lambda = [1 \;\; 1 \;\; 1]^T$ and $\Gamma = [-1 \;\; 0 \;\; 0]^T$. Here, x_b, x_1 and x_2 denote the displacement of the base, 1st floor and 2nd floor, respectively. The matrix Γ identifies the place in which the MR damper is attached, and $\ddot{x}_g$ is the ground acceleration acting on the structure as an external disturbance. By assuming $\xi = [q \;\; \dot{q}]^T$, this equation can be

written in state-space form as follows:

$$\begin{aligned}\dot{\xi} &= \begin{bmatrix} 0 & I \\ -\mathscr{M}^{-1}\mathscr{K} & -\mathscr{M}^{-1}\mathscr{C} \end{bmatrix}\xi + \begin{bmatrix} 0 \\ -\Lambda \end{bmatrix}\ddot{x}_g \\ &+ \begin{bmatrix} 0 \\ \mathscr{M}^{-1}\Gamma \end{bmatrix}F_{mr} \end{aligned} \quad (3)$$

where F_{mr} is the control input acting on the structure.

B. Passive Damping Design

The performance of the MR damper for constant voltages in four intensities of the El Centro earthquake is examined to obtain a baseline for comparison purposes [17]. The structure is excited with $0.2g$, $0.4g$, $0.6g$ and $0.8g$ El Centro earthquakes and the maximum absolute acceleration of the second floor of the structure is determined for constant actuating voltages from 0 to 8 volts. Fig. 3 shows the experimental results for different intensities of El Centro earthquake. It

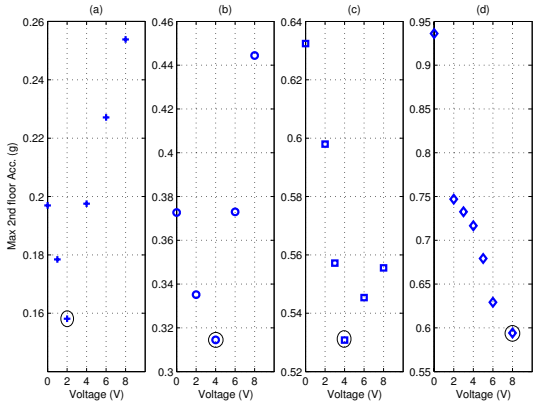

Fig. 3. Optimal passive damping for (a) 0.2 g, (b) 0.4 g, (c) 0.6 g and (d) 0.8 g El Centro earthquakes

is observed that for moderate earthquakes (0.4 g and 0.6 g) the passive damping is *optimal* at $v = 4V$. For lighter earthquakes this value is obtained to be 2V. However, for a destructive 0.8 g earthquake the *optimal* value shifts to 8V. In sum, we choose $v = 4V$ as the *optimal* passive damping which works *optimally* for a wider range of intensities. In reality, there is no information about such an optimal value but in experiments this value is determined for a reasonable comparison.

C. LPV Systems and Modeling

In this section, we present a basic formulation for LPV systems to be used in this paper. An LPV system can be described in the following state-space form [11]

$$\begin{aligned} \dot{x} &= A(\rho)x + B_1(\rho)w + B_2(\rho)u \\ z &= C_1(\rho)x + D_{11}(\rho)w + D_{12}(\rho)u \\ y &= C_2(\rho)x + D_{21}(\rho)w \end{aligned} \quad (4)$$

where x, w and u represent the state vector, the exogenous input vector, and the control input vector, respectively; z and y represent the controlled output and system measurement, respectively. The LPV parameter vector $\rho(t)$ is assumed to be an arbitrary vector $\rho(t) \in \mathscr{F}_{\mathscr{P}}^{v}$, which is not known *a priori* but can be measured in real-time. $\mathscr{F}_{\mathscr{P}}^{v}$ is the set of allowable parameter trajectories defined as

$$\begin{aligned} \mathscr{F}_{\mathscr{P}}^{v} &\triangleq \{\rho \in C(\Re, \Re^s) : \rho(t) \in \mathscr{P}, |\, \dot{\rho}_i(t) \,| \leq v_i, \\ i &= 1, 2, \ldots, s, \forall t \in \Re_+\} \end{aligned}$$

where $\mathscr{P}$ is a compact subset of $\Re^s$, and $\{v_i\}_{i=1}^{s}$ are nonnegative numbers. It is also assumed that $A \in \Re^{n\times n}, B_1 \in \Re^{n\times n_w}, B_2 \in \Re^{n\times n_u}, C_1 \in \Re^{n_z\times n}, D_{11} \in \Re^{n_z\times n_w}, D_{12} \in \Re^{n_z\times n_u}, C_2 \in \Re^{n_y\times n}$ and $D_{21} \in \Re^{n_y\times n_w}$.

The LPV representation of the plant is obtained by describing the system dynamics in a quasi-LPV form. This is achieved by defining new time-varying parameters, which are then regarded as scheduling variables. Since some of the time-varying parameters usually depend on the states, these descriptions are called quasi-LPV [11].

D. Quasi-LPV Modeling of Structure with MR Damper

To proceed with the quasi-LPV modelling of the system, we replace the MR damper force with the modified Bingham model in (1). Therefore, the equation of the motion for the base mass will be rewritten as follows:

$$\begin{aligned} m_b\ddot{x}_b + c_1(\dot{x}_b - \dot{x}_1) + c_b\dot{x}_b + c_0\dot{x}_b e^{-(\frac{\dot{x}_b}{v_0})^2} + k_1(x_b - x_1) + k_b x_b = \\ -f_a \mathtt{sign}(\dot{x}_b) + (-f_b \mathtt{sign}(\dot{x}_b) - c_{0v}\dot{x}_b e^{-(\frac{\dot{x}_b}{v_0})^2})v - m_b\ddot{x}_g \end{aligned}$$

Thus, we can rewrite (2) considering the voltage as the input instead of the damper force.

$$\mathscr{M}\ddot{x} + \mathscr{C}_m\dot{x} + \mathscr{K}x = \Gamma_m v - \mathscr{M}\Lambda\ddot{x}_g \quad (5)$$

where the modified matrices $\mathscr{C}_m$ and Γ_m are defined as follows:

$$\begin{aligned} \mathscr{C}_m &= \begin{bmatrix} c_{11} + \frac{f_a \mathtt{sign}(\dot{x}_b)}{\dot{x}_b} + c_0 e^{-(\frac{\dot{x}_b}{v_0})^2} & c_{12} & 0 \\ c_{12} & c_{22} & c_{23} \\ 0 & c_{23} & c_{33} \end{bmatrix}, \\ \Gamma_m &= \begin{bmatrix} -f_b \mathtt{sign}(\dot{x}_b) - c_{0v}\dot{x}_b e^{-(\frac{\dot{x}_b}{v_0})^2} \\ 0 \\ 0 \end{bmatrix} \end{aligned}$$

where c_{ij}'s are the elements of the system damping matrix $\mathscr{C}$. In order to prevent division by zero in (1,1) element of the matrix $\mathscr{C}_m$, we consider $\frac{\mathtt{sign}(\dot{x}_b)}{\dot{x}_b} = \frac{1}{|\dot{x}_b| + \varepsilon}$, where ε is a positive small value. By substituting the above matrices in (3) and considering the base velocity $\rho = \dot{x}_b$ as the scheduling parameter the following quasi-LPV representation of the system is obtained.

$$\begin{aligned} \dot{\xi} &= \begin{bmatrix} 0 & I \\ -\mathscr{M}^{-1}\mathscr{K} & -\mathscr{M}^{-1}\mathscr{C}_m(\rho) \end{bmatrix}\xi + \begin{bmatrix} 0 \\ -\mathscr{M}^{-1}\Lambda \end{bmatrix}w \\ &+ \begin{bmatrix} 0 \\ \mathscr{M}^{-1}\Gamma_m(\rho) \end{bmatrix}v \end{aligned} \quad (6)$$

It is noted that the base velocity is obtained by low-pass filtering and differentiating the base displacement.

E. LPV Controller Design

The objective of the gain-scheduled output-feedback control problem is to design a dynamic LPV controller with the following state-space representation:

$$\begin{aligned} \dot{x}_K &= A_K(\rho)x_K + B_K(\rho)y \\ u &= C_K(\rho)x_K + D_K(\rho)y, \end{aligned} \tag{7}$$

that ensures the internal stability and a guaranteed induced L_2-gain bound γ on the closed-loop system from exogenous input vector w to the controlled output vector z. The LPV controller (7) is designed via the basic characterization theorem presented in [1]. In our design, we assume that the matrices $\hat{A}_K$, $\hat{B}_K$, $\hat{C}_K$, D_K and X are constant, and the matrix Y is set to be linearly dependent on the scheduling parameter $Y = Y_0 + \rho Y_1$. The scheduling parameter is chosen to be the damper velocity $\rho = \dot{x}_b$ for which $\rho \in [-0.3, 0.3]$ m/s and $\dot{\rho} \in [-5, 5]$ m/s^2. The corresponding synthesis LMIs are solved by gridding the parameter space for ρ over its range of variation following the procedure described in [1].

The LPV controller is designed based on a mixed-sensitivity approach. The design objective is to develop a control strategy to minimize the induced L_2 norm of the closed-loop system transfer functions from the external disturbance to the controlled outputs selected appropriately. Since we have a regulation problem tracking is not an issue and therefore it makes sense to shape the closed-loop transfer functions S and KS [14]. We recall that S is the transfer function between the disturbance $w = \ddot{x}_g$ and the output, and KS the transfer function between w and the control signal. The controlled output vector is assumed to be $z = [z_1, z_2]^T = [W_s y, -W_u u]^T$.

The absolute acceleration of the second floor is set to be the measured output $y = -(\ddot{x}_2 + \ddot{x}_g)$. The dynamic weights for LPV design are chosen to be $W_u = \frac{1.2\times10^{-4}s}{s+40}$ and $W_s = \frac{1}{s^2+s+10}$, where W_u is the weight on the control signal (desired damping force) and selected to be a high pass filter. On the other hand, W_s is the weight on y. This weight begins rolling off before the first natural frequency of the system which is about 13 rad/s. The system matrices in (4) are determined correspondingly for the augmented plant with the dynamic weights, where A and B_2 are the only matrices dependent on the scheduling parameter.

For practical reasons, a saturation limit of V_{max}=8V is considered for the MR damper device. Therefore, the commanded force and the force produced by the applied voltage may not be the same due to saturation constraint. It is known that saturation can deteriorate the closed-loop performance of the system [8]. In order to overcome this problem the LPV controller is combined with a classical anti-windup scheme [4] to alleviate the saturation effect.

V. Experimental Results of MR Damper Control

As discussed earlier, a shaking table is used to simulate the earthquake and excite the structure. El Centro and Northridge earthquakes with two different intensities are chosen for structural response comparisons. There is always a tradeoff in designing the base isolation system between decreasing the structure acceleration and base drift. However, the main concern is about structure acceleration and base drift should not exceed some limits of displacement to prevent colliding with the base foundation. The structural responses for 0V passive damper and LPV control, and the control input are illustrated in Fig. 4. The structural responses due to 0.6 g El

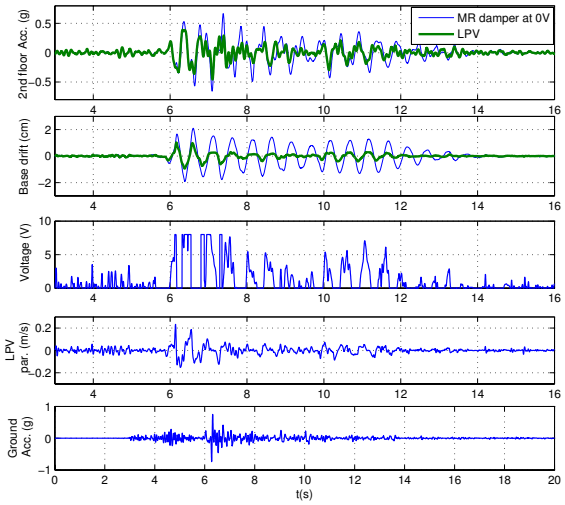

Fig. 4. Northridge 0.7 g ground excitation, the structural responses for 0V damper and LPV control, LPV voltage and its parameter variations

Centro earthquake corresponding to the LPV controller and "without damper" case are also shown in Fig. 5. The "without damper" case represents the response of the base-isolated structure without any additional damping system. Tables 1

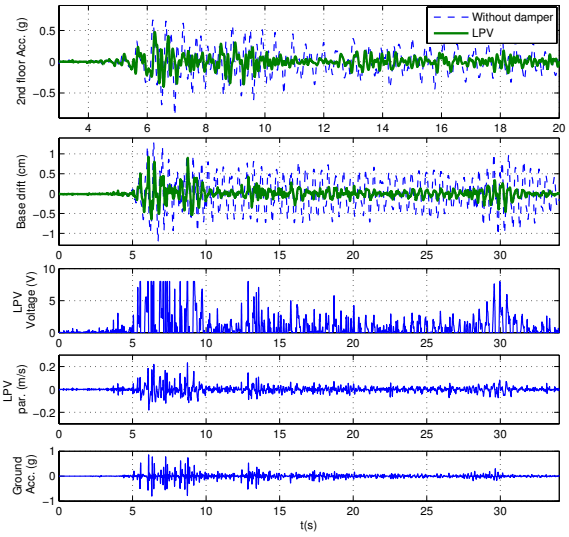

Fig. 5. El Centro 0.6 g ground excitation, LPV control voltage and the second floor acceleration responses for without damper case and LPV controller

TABLE I

MAXIMUM EXPERIMENTAL RESPONSES DUE TO SIMULATED EARTHQUAKES

	El Centro (0.2 g)	El Centro (0.6 g)	Northridge (0.3 g)	Northridge (0.7 g)
Ground acceleration (cm/s^2)				
	196.2	590.5	295.3	688.7
Second floor acceleration (cm/s^2)				
Without damper	250.5	838.7	312.3	840.3
Passive damping	193.8	510.3	204.6	500.1
LPV control	137.5	464.7	180.2	454.9
Base drift (cm)				
Without damper	0.4309	1.282	0.6089	1.531
Passive damping	0.2285	0.9130	0.3639	1.1857
LPV control	0.3040	0.9277	0.4182	1.016

TABLE II

ROOT MEAN SQUARE (RMS) VALUE OF EXPERIMENTAL RESPONSES DUE TO SIMULATED EARTHQUAKES

	El Centro (0.2 g)	El Centro (0.6 g)	Northridge (0.3 g)	Northridge (0.7 g)
Ground acceleration (cm/s^2)				
	26.22	78.68	35.33	82.67
Second floor acceleration (cm/s^2)				
Without damper	44.39	176.1	78.29	215.82
Passive damping	32.56	76.48	31.68	73.95
LPV control	23.79	76.41	28.63	72.41
Base drift (cm)				
Without damper	0.0940	0.3933	0.2048	0.5702
Passive damping	0.0242	0.1054	0.0367	0.1295
LPV control	0.0337	0.1250	0.0466	0.1377

and 2 present the maximum and RMS experimental structural responses due to simulated earthquakes with different intensities. In case of the second floor absolute acceleration, the LPV controller shows up to 30% smaller peaks for weak earthquakes and up to 10% smaller peaks for strong earthquakes compared to the passive damping. In the case of base drift the passive damping shows improved results. However, this control scenario is not realistic and practically a constant actuating voltage cannot be optimal for all types of earthquakes with varying intensities as mentioned before. Considering all the maximum and RMS results, the LPV controller is determined to be an optimal realistic control strategy compared to passive damping.

VI. CONCLUSION

Parameter identification and LPV control of an MR damper with stiction effect was studied in this paper. A modified Bingham model was introduced to capture the stiction effect and velocity-dependent damping of the MR damper. Both identification and control were performed on the same setup which reduced the required experimental effort. After identifying the parameters, an LPV controller based on the modified Bingham model was designed to directly command the MR damper voltage. The quasi-LPV model of the combined structure and damper was presented by selecting the damper velocity as the scheduling parameter. The LPV controller was obtained by solving a set of LMIs over the range of the variations of the parameter. For practical reasons, a saturation limit of 8V was assumed to actuate the MR damper. Therefore, a classical anti-windup scheme was employed to eliminate the effect of saturation and keep the output voltage within the saturation bound. An optimal passive damping was also obtained for El Centro earthquake with different intensities for comparison purposes. The performance of the LPV controller was investigated experimentally for El Centro and Northridge earthquakes with different intensities. The experimental results showed the improved performance of our controller design approach in terms of maximum acceleration and RMS values for the structure response.

REFERENCES

[1] P. Apkarian and R. J. Adams, "Advanced gain-Scheduling techniques for uncertain systems," *IEEE Tran. on Control Systems Technology*, vol. 6, Issue 1, pp. 21-32, 1998.

[2] A. Do, O. Sename and L. Dugard, "An LPV Control Approach for Semi-active Suspension Control with Actuator Constraints," *in Proc. American Control Conference*, pp. 4653-4658, Baltimore, USA, 2010.

[3] S. J. Dyke, *Acceleration Feedback Control Strategies for Active and Semi-active Control Systems: Modeling, Algorithm Development, and Experimental Verification*, Ph.D. Thesis, University of Notre Dome, 1996.

[4] C. Edwards and I. Postlethwaite, "Anti-windup and Bumpless Transfer Schemes," *in Proc. UKACC International Conference on Control*, pp. 394-399, Exeter, UK, 1996.

[5] P. Gahinet and P. Apkarian, "A linear matrix inequality approach to H_∞ control," *Int J. Robust and Nonlinear Control*, 4(4), pp. 421-448, 1994.

[6] D. Haiping, K. Y. Sze and J. Lam, "Semi-active H_∞ Control of Vehicle Suspension with Magneto-rheological Dampers," *Journal of Sound and Vibration*, vol. 283, pp. 981-996, 2005.

[7] R. Jimenez and L. Alvarez-Icaza, "LuGre Friction Model for a Magnetorheological Damper," *Structural Control and Health Monitoring*, vol. 12, pp. 91-116, 2005.

[8] V. Kapila and K. M. Grigoriadis (eds), *Actuator Saturation Control*, Marcel Dekker, New York, 2003.

[9] H. Olsson, K. J. Astrom, C. C. de Wit, M. Gafvert and P. Lischinsky, "Friction Models and Friction Compensation," *European Journal of Control*, vol. 4, No. 3, pp. 176-195, 1998.

[10] C. Poussot-Vassal, O. Sename, L. Dugard, P. Gaspar, Z. Szabo and J. Bokor, "A New Semi-Active Suspension Control Strategy Through LPV Technique," *Control Engineering Practice*, vol. 16, pp. 1519-1534, 2008.

[11] W. J. Rugh and J. S. Shamma, "Research on gain scheduling," *Automatica*, vol. 36, pp. 1401-1425, 2000.

[12] C. Sakai, T. Terasawa and A. Sano, "Integration of Bilinear H_∞ Control and Adaptive Inverse Control for Semi-Active Vibration Isolation of Structures," *in Proc. 44th IEEE Conference on Decision and Control, and European Control Conference*, pp. 5310-5316, Seville, Spain, 2005.

[13] F. A. Shirazi, J. Mohammadpour and K. M. Grigoriadis, "An Integrated Approach for Parameter Identification and Semi-active Control of MR Dampers," *in Proc. American Control Conference*, pp. 720-725, Baltimore, USA, 2010.

[14] S. Skogestad and I. Postlethwaite, *Multivariable Feedback Control Analysis and Design*, Wiley, 2005.

[15] B. F. Spencer Jr., S. J. Dyke, M. K. Sain and J. D. Carlson, "Phenomenological Model of a Magnetorheological Damper", *ASCE Journal of Engineering Mechanics*, vol. 123, No 3, pp. 230-238, 1997.

[16] G. Yang, *Large-Scale Magnetorheological Fluid Damper for Vibration Mitigation: Modeling, Testing and Control*, University of Notre Dame, Indiana, 2001.

[17] H. Yoshioka, J. C. Ramallo and B. F. Spencer Jr., "Smart Base Isolation Strategies Employing Magnetorheological Dampers," *Journal of Engineering Mechanics*, vol. 128, No 5, pp. 540-551, 2002.

[18] M. Zapateiro, *Semiactive Control Strategies for Vibration Mitigation in Adaptronic Structures Equipped with Magnetorheological Dampers*, PhD Thesis, University of Girona, 2009.